J|A|C|S ARTICLES

Published on Web 05/14/2009

Femtosecond Time-Resolved Stimulated Raman Reveals the Birth of Bacteriorhodopsin's J and K Intermediates

Sangdeok Shim, Jyotishman Dasgupta, and Richard A. Mathies*

Department of Chemistry, University of California, Berkeley, California 94720

Received November 22, 2008; E-mail: rich@zinc.cchem.berkeley.edu

Abstract: Light-activated proton translocation in halobacteria is driven by photoisomerization of the retinal chromophore within the membrane-bound protein bacteriorhodopsin. The molecular mechanism of this process has been widely debated due to the absence of structural information on the time scale of the reactive dynamics (the initial 0.1−1 ps). Here we use tunable femtosecond stimulated Raman spectroscopy to obtain time-resolved resonance Raman vibrational spectra of bacteriorhodopsin's key J and K photoisomerization intermediates. The appearance of the J state is delayed by ∼150 fs relative to the zero of time and rises after this dwell with a 450 fs time constant. The J state is characterized by a 16 cm^{-1} red-shifted C=C stretch, which blue shifts by 5 cm^{-1} coincident with the rise of the K state. The delayed 3 ps rise of the C_{15}−H HOOP mode with enhanced intensity in K reveals the appearance of strain near the Schiff's base once the 13-*cis* configuration is fully formed. The delay in the initial appearance of J is assigned to nuclear dynamics on the excited state that precede the formation of the proper geometry for reactive internal conversion.

Introduction

The transduction of solar energy into chemical work by biomolecules is the paradigm that powers life on earth.[1] Bacteriorhodopsin (bR), a protein found in the purple membrane of *Halobacterium salinarum*, is an important example of this photosynthetic process. Upon light absorption, bR efficiently creates a proton gradient across the membrane which drives ATP synthesis.[2] The retinal chromophore within bR captures the photon energy by rapidly isomerizing from *all-trans* to a *cis* configuration about the C_{13}=C_{14} double bond (Figure 1).[3] Elucidating the molecular mechanism of this 65% efficient process is fundamental to the understanding of photoisomerization reactions, and may ultimately lead to the development of artificial light-activated conformational switches and energy capture devices.[4,5]

Because the primary event in bR occurs on the subpicosecond time scale, ultrafast pump−probe transient electronic[6−8] and vibrational spectroscopies[9,10] have been used to study the temporal and structural evolution of bR's early intermediates.[11] Figure 1 depicts the photoisomerization in bR and the reaction intermediates with their characteristic absorption maxima. The Franck−Condon state (H) decays to an excited state intermediate

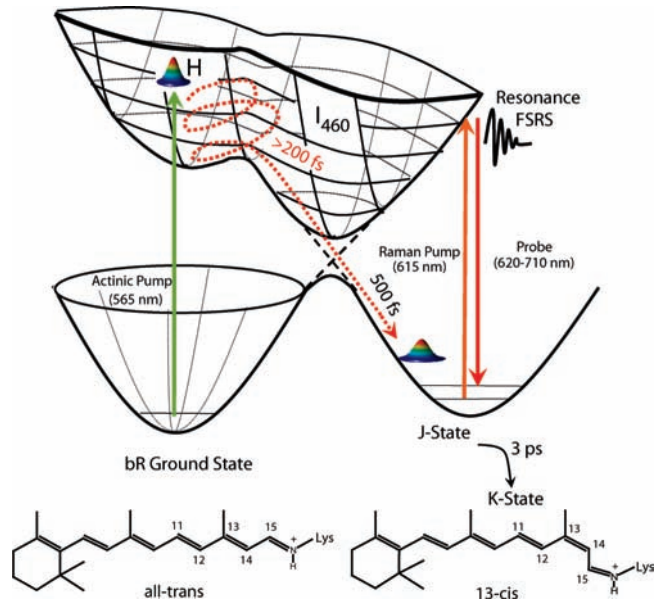

Figure 1. Schematic of the photoisomerization process in bacteriorhodopsin. A femtosecond actinic pulse at 565 nm excites the system to H where it undergoes >200 fs of nuclear dynamics before forming I_{460}. The resonance conditions induced by the 615 nm Raman pump (R_{pu}) and the 620−710 nm Raman probe (R_{pr}) pulses selectively enhance the ground state photoproduct and suppress resonance emission interference from the excited states.

(1) Lewis, N. S.; Nocera, D. G. *Proc. Natl. Acad. Sci. U.S.A.* **2006**, *103*, 15729–15735.
(2) Subramaniam, S.; Henderson, R. *Nature* **2000**, *406*, 653–657.
(3) Mathies, R. A.; Lin, S. W.; Ames, J. B.; Pollard, W. T. *Annu. Rev. Biophys.* **1991**, *20*, 491–518.
(4) Sinicropi, A.; et al. *Proc. Natl. Acad. Sci. U.S.A.* **2008**, *105*, 17642–17647.
(5) Hampp, N. *Chem. Rev.* **2000**, *100*, 1755–1776.
(6) Kahan, A.; Nahmias, O.; Friedman, N.; Sheves, M.; Ruhman, S. *J. Am. Chem. Soc.* **2007**, *129*, 537–546.
(7) Kobayashi, T.; Saito, T.; Ohtani, H. *Nature* **2001**, *414*, 531–534.
(8) Haran, G.; Wynne, K.; Xie, A. H.; He, Q.; Chance, M.; Hochstrasser, R. M. *Chem. Phys. Lett.* **1996**, *261*, 389–395.
(9) Doig, S. J.; Reid, P. J.; Mathies, R. A. *J. Phys. Chem.* **1991**, *95*, 6372–6379.
(10) Diller, R.; Maiti, S.; Walker, G. C.; Cowen, B. R.; Pippenger, R.; Bogomolni, R. A.; Hochstrasser, R. M. *Chem. Phys. Lett.* **1995**, *241*, 109–115.
(11) Sundstrom, V. *Annu. Rev. Phys. Chem.* **2008**, *59*, 53–77.

10.1021/ja809137x CCC: $40.75

I_{460}[12] with a blue-shifted 460 nm absorption. Although the structure of the chromophore in I_{460} remains unclear, recent work has shown that bR with locked retinal analogues show photoinduced spectral changes that are similar to that of ordinary bR at early times. The similarity of the initial transient spectral evolution of both native and these artificial pigments indicates that the ultrafast process from H to I_{460} does not yet involve C_{13}═C_{14} torsion.[13] Mathies and co-workers showed that the J intermediate which appears in 500 fs eventually leads to the fully isomerized K photoproduct in 3 ps.[14] The high resolution X-ray structure of K trapped at low temperature confirms that the isomerization is complete in the K intermediate.[15] Using impulsive vibrational spectroscopy, Kobayashi and co-workers concluded that the C_{13}═C_{14} bond in the I state is distorted and that the isomerization is nearly complete in the photoproduct J.[7] Electric field-induced optical absorption broadening demonstrated that the dipole moment of the retinal chromophore changes by ~13 D upon photoexcitation, quantitating the immediate charge separation in the FC state.[16] The transient changes in the electronic absorption after retinal excitation of the excitonically coupled tryptophan residues Trp86/Trp182 have temporally resolved this charge separation event.[17−19]

Despite this detailed knowledge of the electronic changes that occur when the retinal chromophore in bR is excited, the nuclear dynamics during the ultrafast isomerization process are not well-known. Mid-IR spectroscopy by Diller and co-workers recently probed the ethylenic region and assigned a red-shifted C═C stretch to the J intermediate while concluding that the isomerization is complete by 500 fs.[20] However, these experiments did not identify the key structural changes of the chromophore backbone during the isomerization due to the limited range of the vibrational data (1400−1800 cm^{-1}) as well as masking by protein vibrations.

Resonance Raman spectra of both native and isotopically substituted retinal derivatives in bR have been used to characterize the Raman active vibrational modes along with their respective Raman cross sections.[21−25] Time-resolved Raman spectroscopy has also been used to interrogate the J and K intermediates.[9] However, the limited picosecond time-resolution of these experiments convolved the J-state vibrations with the K-state Raman spectrum, making an unambiguous structural analysis difficult.[9,26] With the advent of femtosecond stimulated Raman spectroscopy (FSRS) it is now possible to probe structural intermediates formed in the bR photocycle with much higher temporal (~50 fs) and spectral resolution (<10 cm^{-1}).[27−29] In addition, the recent development of a tunable Raman pump pulse has extended time-resolved FSRS to the resonance Raman domain.[30,31] With this advance it is possible to select Raman pump and probe wavelengths distant from the stimulated emission region and the ground state bleaching band. This capability inherently reduces the overlapping hot luminescent features seen in previous off-resonance FSRS studies on bR, which masked the critical structural transitions during the initial 500 fs of this reaction.[32,33]

Herein, we report resonance FSRS spectra of bR using a tunable Raman pump pulse to resonantly excite the photoproduct and obtain high quality time-resolved Raman spectra. The appearance of the photoproduct J is resolved as well as its structural evolution to the photoproduct K on the ground state potential energy surface. The frequency shift of the ethylenic mode over time reveals the delocalization in the J state caused by the charge transfer from the Schiff's base to the polyene backbone. Using these time-resolved vibrational spectra, the appearance and structure of the J-state is temporally resolved along with its structural evolution to a more planar C_{13}═C_{14} *cis*-geometry in the K intermediate.

Materials and Methods

Bacteriorhodopsin extracted from *Halobacterium salinarum* cultures was generously provided by Prof. Roberto Bogomolni (U.C., Santa Cruz). The bR solution was prepared by resuspending the pellet of purple membrane in 5 mM *N*-2-hydroxyethylpiperazine-*N*″-2-ethanesulfonic acid (HEPES) buffered at pH 7.4 using an eppendorf homogenizer pestle. The 12 OD/cm (at 568 nm) sample was light-adapted with a desk lamp while on ice for 15 min, and adaptation was maintained by constant illumination with a fluorescent bulb. The UV−vis absorption exhibited no changes throughout the experiment. The sample was flowed in a 1 mm flow cell at a sufficient rate to ensure a fresh volume for each shot.

The tunable FSRS apparatus and methods have been described in detail elsewhere.[30] In brief, the output of a Ti:sapphire regenerative amplifier (Spitfire, Spectra Physics) is modified to produce the three pulses needed to obtain time-resolved FSRS spectra. The 565 nm actinic pulse (<50 fs, 100 nJ, ~80 μm beam diameter at the sample) generated by a noncollinear optical parametric amplifier (NOPA) initiates the bR photocycle. To optimize the resonance Raman effect and to avoid undesirable nonlinear interference, we chose the Raman and probe pulses in the visible range within the absorption bands of bR's J and K intermediates. The stimulated Raman transitions are driven by a 615 nm Raman pulse (0.8 ps, 25 cm^{-1}, 100 nJ) produced by a narrow bandwidth optical parametric

(12) Kahan, A.; Nahmias, O.; Friedman, N.; Sheves, M.; Ruhman, S. *J. Am. Chem. Soc.* **2007**, *129*, 537–546.
(13) Ye, T.; Friedman, N.; Gat, Y.; Atkinson, G. H.; Sheves, M.; Ottolenghi, M.; Ruhman, S. *J. Phys. Chem. B* **1999**, *103*, 5122–5130.
(14) Mathies, R. A.; Cruz, C. H. B.; Pollard, W. T.; Shank, C. V. *Science* **1988**, *240*, 777–779.
(15) Edman, K.; Nollert, P.; Royant, A.; Belrhali, H.; Pebay-Peyroula, E.; Hajdu, J.; Neutze, R.; Landau, E. M. *Nature* **1999**, *401*, 822–826.
(16) Mathies, R.; Stryer, L. *Proc. Natl. Acad. Sci. U.S.A.* **1976**, *73*, 2169–2173.
(17) Groma, G. I.; Hebling, J.; Kozma, I. Z.; Varo, G.; Hauer, J.; Kuhl, J.; Riedle, E. *Proc. Natl. Acad. Sci. U.S.A.* **2008**, *105*, 6888–6893.
(18) Schenkl, S.; van Mourik, F.; Friedman, N.; Sheves, M.; Schlesinger, R.; Haacke, S.; Chergui, M. *Proc. Natl. Acad. Sci. U.S.A.* **2006**, *103*, 4101–4106.
(19) Schenkl, S.; van Mourik, F.; van der Zwan, G.; Haacke, S.; Chergui, M. *Science* **2005**, *309*, 917–920.
(20) Herbst, J.; Heyne, K.; Diller, R. *Science* **2002**, *297*, 822–825.
(21) Smith, S. O.; Braiman, M. S.; Myers, A. B.; Pardoen, J. A.; Courtin, J. M. L.; Winkel, C.; Lugtenburg, J.; Mathies, R. A. *J. Am. Chem. Soc.* **1987**, *109*, 3108–3125.
(22) Smith, S. O.; Myers, A. B.; Braiman, M.; Pardoen, J. A.; Winkel, C.; Mulder, P. P. J.; Lugtenburg, J.; Mathies, R. *Biophys. J.* **1984**, *45*, A209–A209.
(23) Myers, A. B.; Harris, R. A.; Mathies, R. A. *J. Chem. Phys.* **1983**, *79*, 603–613.
(24) Mathies, R. *Methods Enzymol.* **1982**, *88*, 633–643.
(25) Curry, B.; Broek, A.; Lugtenburg, J.; Mathies, R. A. *J. Am. Chem. Soc.* **1982**, *104*, 5274–5286.
(26) Atkinson, G. H.; Ujj, L.; Zhou, Y. *J. Phys. Chem. A* **2000**, *104*, 4130–4139.
(27) Kukura, P.; McCamant, D. W.; Mathies, R. A. *Annu. Rev. Phys. Chem.* **2007**, *58*, 461–488.
(28) McCamant, D. W.; Kukura, P.; Yoon, S.; Mathies, R. A. *Rev. Sci. Instrum.* **2004**, *75*, 4971–4980.
(29) Yoshizawa, M.; Kurosawa, M. *Phys. Rev. A: At., Mol., Opt. Phys.* **1999**, *61*, 013808.
(30) Shim, S.; Mathies, R. A. *J. Phys. Chem. B* **2008**, *112*, 4826–4832.
(31) Shim, S.; Mathies, R. A. *Appl. Phys. Lett.* **2006**, *89*, 121124.
(32) Frontiera, R. R.; Shim, S.; Mathies, R. A. *J. Chem. Phys.* **2008**, *129*, 064507.
(33) McCamant, D. W.; Kukura, P.; Mathies, R. A. *J. Phys. Chem. B* **2005**, *109*, 10449–10457.

amplifier (NB-OPA) together with a broadband probe pulse (<50 fs, 620−710 nm, <10 nJ) generated by focusing the fundamental output in a sapphire substrate.[31] The actinic and probe pulse durations are minimized with SF 10 prism compressors. The instrument response is determined by cross-correlation between the actinic and probe pulses. Sum frequency generation in a 2 mm BBO crystal between the actinic and probe pulses reveals an instrument response of ∼70 fs. All three pulses are noncollinearly focused onto the flow cell containing the bR suspension. After the sample, the probe pulse is dispersed onto a dual photodiode array.

FSRS gain spectra are calculated by the equation that includes the contributions from conventional transient absorption caused by the actinic and probe pulses,[30]

$$\text{Raman gain} = \frac{[(\text{probe} + \text{actinic} - \text{bkgnd})/(\text{ref} - \text{bkgnd})]_{\text{Raman pulse on},\Delta t}}{[(\text{probe} + \text{actinic} - \text{bkgnd})/(\text{ref} - \text{bkgnd})]_{\text{Raman pulse off},\Delta t}}$$

where bkgnd refers to the detector background measured with all the beams blocked and Δt represents time delay between the actinic and Raman probe pulse. Using this modified equation, the complex sloping baseline caused by the strong transient absorption can be minimized.

The data reduction procedure is illustrated for the 1 ps spectrum in Figure 2. To remove the contribution from the unreactive molecules and to produce reliable Raman spectra of the bR photoproducts, it was crucial to quantitatively remove the broad baseline as well as the Raman scattering from the bR ground state. The ground state spectrum (A) was obtained without the actinic pulse. By employing the actinic pulse, the transient Raman spectrum (B) containing features due to the photoproduct along with the reduced ground state features is produced. The photoproduct spectrum at a given time delay is generated by subtracting a fraction of the ground state spectrum from the raw spectrum (B $- f \times$ A). A scaling factor f was set so that first the resulting difference spectrum reveals the negative features at the locations of prominent bR bands at 1008 and 1527 cm^{-1} and doublet around 1200 cm^{-1}. The scaling factor was then reduced until these negative peaks are just eliminated (see the lower panel). Finally, a spline fit to the broad baseline was used to produce the background free spectrum of the photoproduct.

Results

Figure 3 presents selected resonance FSRS spectra of the bR photoproducts after 565 nm photoexcitation compared with the ground state spectrum. To obtain a well-defined resonance Raman spectrum of the photoproduct, the characterization of the ground state spectrum is critical. The ground state spectrum exhibits three major peaks: the ethylenic C═C stretch at 1527 cm^{-1}, the fingerprint C−C stretch doublet at 1170 and 1203 cm^{-1}, and the methyl rock at 1008 cm^{-1}. Although their intensities are weak, the hydrogen out-of-plane (HOOP) mode at 952 cm^{-1}, the C−C−H in-plane rocking modes at 1270 and 1335 cm^{-1}, the in-plane deformation mode at 1453 cm^{-1}, and the C═N stretch at 1640 cm^{-1} are also visible. All observed vibrational frequencies are in agreement with previous resonance Raman studies.[25,34]

Our resonance FSRS spectra of the bR photoproducts are different from the ground state spectrum even at the earliest time point at 50 fs, and exhibit three major vibrational features at 1004 cm^{-1} (C−CH_3), 1190 cm^{-1} (C−C), and 1510−1525 cm^{-1} (C═C). Comparing the ethylenic peaks of the ground state spectrum and the photoproduct spectra, it is clear that this vibration is downshifted at all time delays and its frequency

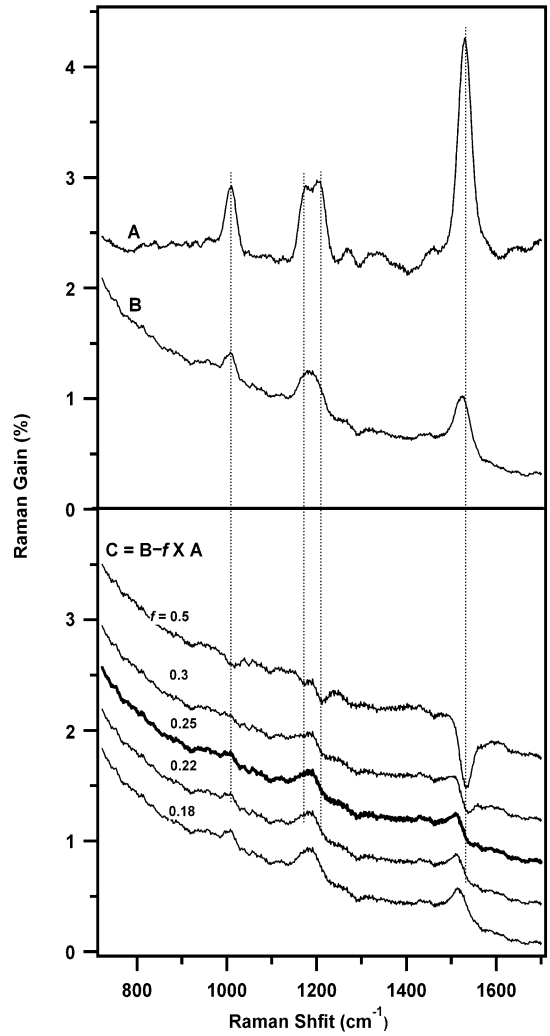

Figure 2. Data reduction procedure for time-resolved FSRS spectra of bacteriorhodopsin. The ground state spectrum (A) and the unprocessed spectrum at 1 ps time delay (B) were obtained without and with the actinic pulse, respectively (top panel). To obtain an excited-state-only spectrum (C) a fraction of the ground state spectrum ($f \times$ A) is subtracted from the raw spectrum (B) (bottom panel). The scaling factor was determined by first oversubtracting until negative features were observed at prominent bands (dotted lines), and then reducing f until these negative peaks were just eliminated. A comparison of the resulting spectra obtained by varying the scaling factor (f) is also displayed. In this example, the best scaling factor of 0.25 was determined (bold spectrum).

exhibits a dynamic shift over time. The ground state fingerprint peaks at 1170 and 1203 cm^{-1} transition into a single broad peak at ∼1189 cm^{-1} at the earliest time point. A HOOP mode at 962 cm^{-1}, initially visible in the 600 fs spectrum, grows to maximum amplitude with a time constant of ∼3 ps and barely changes beyond 5 ps. Particularly, the 5 and 10 ps spectra are consistent with previous picosecond time-resolved resonance Raman studies revealing (1) the ethylenic downshift from 1527 to ∼1517 cm^{-1}, which is regarded as a marker of the 13-*cis* photoproduct; (2) an intense peak at 1189 cm^{-1}, which has been assigned to the C_{10}−C_{11} stretch in 13-*cis* photoproduct; (3) and a large HOOP at 962 cm^{-1}, assigned to the C_{15}−H HOOP, with intensity comparable to the methyl rocking mode at 1004 cm^{-1}.[34]

Figure 4 presents the kinetics of the peak area and frequency shift of the ethylenic band over time. The area and center of this peak were determined by fitting to a Gaussian line shape function. The time evolution of peak area (Figure 4A) was

(34) Braiman, M.; Mathies, R. *Proc. Natl. Acad. Sci. U.S.A.* **1982**, *79*, 403–407.

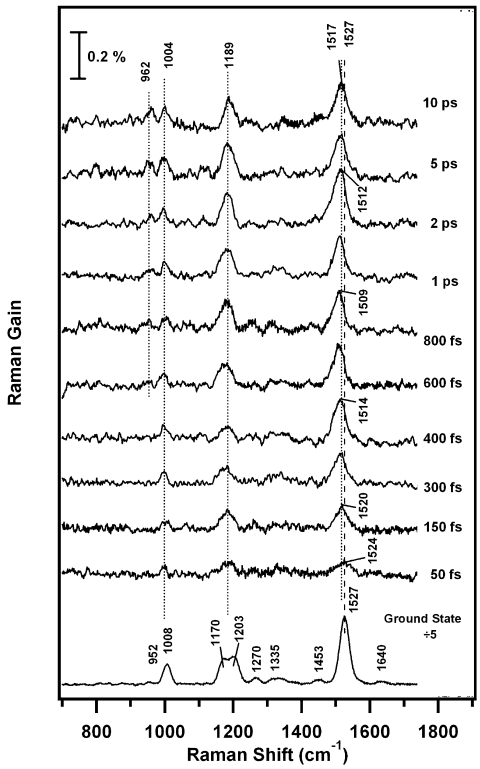

Figure 3. Selected time-resolved FSRS spectra at various time delays after photoexcitation with a 50 fs actinic pulse at 565 nm. Spectra were obtained using 615 nm Raman excitation, which is resonant with the J and K photoproducts. Peaks attributed to the photoproduct are indicated with the dashed vertical lines. The dynamic peak shift of the ethylenic stretch mode from 50 fs to 10 ps is indicated.

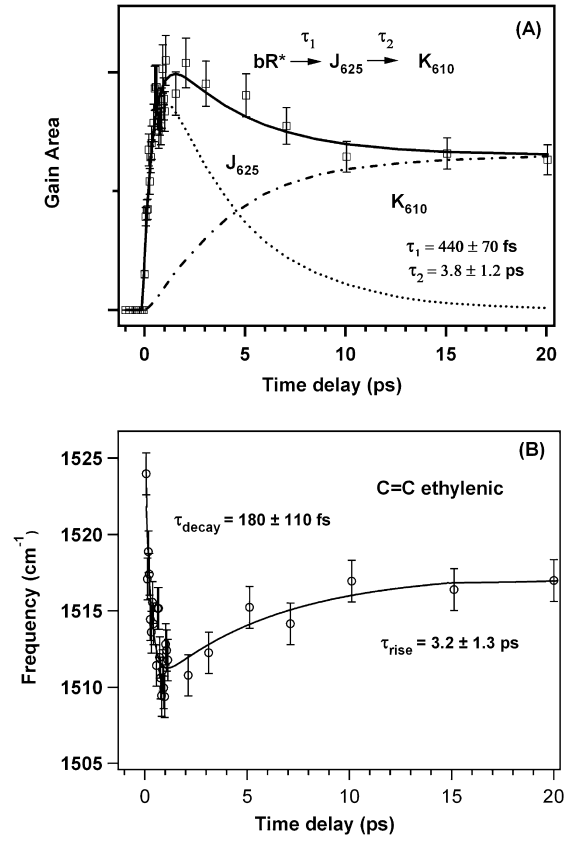

Figure 4. (A) Kinetics of bR's C═C ethylenic peak areas at ∼1518 cm^{-1}. Solid line is a fit to a convolution of the 70 fs instrument response with an exponential molecular response exhibiting a ∼450 fs risetime and a single 4 ps exponential decay. Corresponding population changes in the J (dotted line) and K (dash-dotted line) intermediates are also displayed. (B) Time-dependent frequency shift of the C═C ethylenic peaks of bR, exhibiting a ∼180 fs reduction followed by a ∼3 ps rise.

determined using a nonlinear least-squares fit to a convolution of the 70-fs instrument response function and a multiexponential function. The ethylenic peak grows in until 1−2 ps and decays with time constants of 450 fs and 4 ps, respectively. These time constants are in excellent agreement with various transient absorption measurements of the time scale for the formation of the J and K intermediates.[14,35−37]

Figure 4B illustrates that the frequency of the ethylenic mode red-shifts rapidly to ∼1512 cm^{-1} over the first picosecond and then blue-shifts rather slowly up to ∼1517 cm^{-1} at later time delays. Fitting the temporal dynamics of the frequency change to a double exponential reveals that the peak red-shifts from 1525 to 1512 cm^{-1} with a 180 fs time constant and then blue-shifts to 1517 cm^{-1} with a 3 ps time constant. Because the vibrational frequency of the ethylenic mode correlates inversely with the increase in retinal absorption wavelength,[38] it can be used as an indirect gauge of the absorption maximum of the structural intermediates during the bR photocycle as a function of time.[39] Using this correlation, the minimal 1512 cm^{-1} frequency predicts an absorption maximum of around 628 nm (J), and the 1517 cm^{-1} frequency correlates with a 610 nm (K) absorption maximum, as expected. The best-fit peak positions were used for the estimation of the absorption maximum to minimize the impact of the experimental error.

The traces in Figure 4 exhibit a delayed onset (τ_0) compared to the zero time delay ($\Delta t = 0$), which is set by the cross-correlation. The delayed onset of these signals provides information on the timing of the molecular response to the optical pump pulse during the photoinduced reaction. Because the decrease in the population of the ground state by the optical pump pulse follows its profile, the ground state bleaching transient absorption (TA) feature is a convolution of the instrument response with the molecular response function. It is thus expected that this TA signal will be 50% complete at the true zero of time. On the other hand, the observation of a delayed onset of a signal is an indication that there is an intermediate process between vertical excitation and the production of the observed species.

To explore this question more quantitatively, we performed TA measurements within the FSRS probe window by blocking the Raman pump pulse without any change of experimental conditions. Traces for the TA appearance signals probed at 660 nm are presented in Figure 5 along with the FSRS ethylenic mode appearance. It is evident that the TA signals begin to appear significantly earlier than the FSRS signals. To quantify the delayed timing of the FSRS signals relative to the TA signals, the onsets of both traces were fit to a convolution with our 70 fs instrument response function, in which the onset (τ_0) was allowed to vary freely. The FSRS traces rise 150 fs after

(35) Nuss, M. C.; Zinth, W.; Kaiser, W.; Kolling, E.; Oesterhelt, D. *Chem. Phys. Lett.* **1985**, *117*, 1–7.
(36) Polland, H. J.; Franz, M. A.; Zinth, W.; Kaiser, W.; Oesterhelt, D. *Biochim. Biophys. Acta* **1986**, *851*, 407–415.
(37) Sharkov, A. V.; Pakulev, A. V.; Chekalin, S. V.; Matveetz, Y. A. *Biochim. Biophys. Acta* **1985**, *808*, 94–102.
(38) Callender, R.; Honig, B. *Annu. Rev. Biophys. Bioenerg.* **1977**, *6*, 33.
(39) Aton, B.; Callender, R. H.; Becher, B.; Ebrey, T. G. *Biochemistry* **1977**, *16*, 2995–2999.

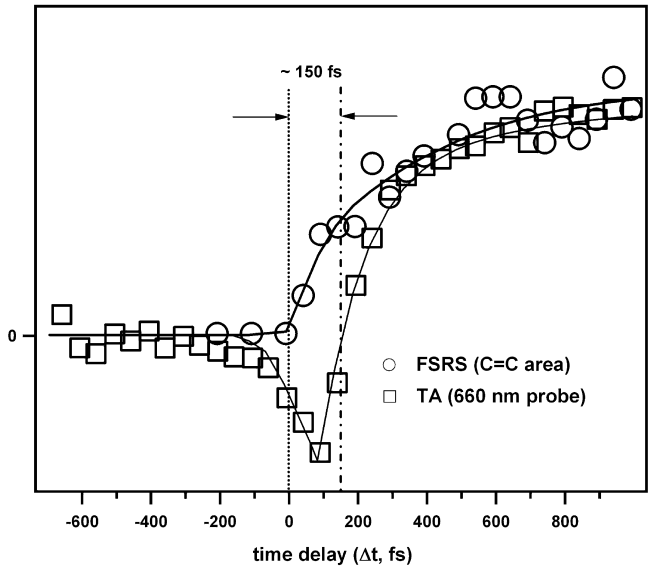

Figure 5. Comparison of the onset of FSRS (○) and transient absorption (TA, □) traces in the primary bR photoproduct production. Transient absorption was measured by blocking the Raman pump pulse without any changes in experimental conditions. The onsets of each trace were determined by fitting to a convolution with our 70 fs instrument response function, in which the time-zero (τ_0) was allowed to vary freely. The dotted and dash-dotted lines indicate the τ_0 of the FSRS and TA signals. The 150 fs delayed appearance of the FSRS signals compared to the TA signals is evident.

the TA signals indicating an intermediate molecular process on the excited state that lies between Franck−Condon excitation and the onset of reactive internal conversion.

Discussion

Femtosecond time-resolved vibrational spectra of the retinal chromophore during the photoisomerization process in bacteriorhodopsin provide new insight on the reaction dynamics and the photocycle intermediate structures. In our previous FSRS studies on bR, interfering nonlinear signals caused by resonance of the 800 nm Raman pump with the stimulated emission band dominated the data observed in the first picosecond.[33] These dispersive vibrational signals arise from hot luminescence terms caused by the population created through two pump field interactions with the excited state.[32] Although the Raman initiated nonlinear emission (RINE) signals provided a measure of the excited state evolution out of Franck−Condon region (∼250 fs), they prevented the direct monitoring of the initial formation and evolution of the primary ground state photoproduct.[33] The key advance presented here is the ability to use a tunable Raman pump wavelength to enable measurement of the Raman transitions in a spectral region that avoids stimulated emission interference. As expected, by using a 615 nm Raman pump, no dispersive RINE signals were observed and the resonance Raman spectra of the photoproducts were obtained at time delays from 0 to 800 fs for the first time.

The FSRS spectra presented here are assigned to the J and K ground state intermediates. The 615 nm Raman pump is on resonance with the J and K absorptions at 625 and 610 nm, respectively, while it is off-resonant with the excited state, with the Franck−Condon state H, and the emissive state I (see Figure 1). Compared to previous NIR FSRS spectra of the photoproduct at 5 ps time delay,[33] the resonance enhancement in our experiments is on the order of 3-fold, confirming that the Raman pump and probe are enhancing J and K scattering.

Previous steady state Raman studies have shown that a powerful method of characterizing the interaction of the retinal chromophore with its protein environment is by measuring the frequency of the C=C stretch mode.[38] The ethylenic mode is sensitive to the degree of net positive charge delocalization from the Schiff's base out to the polyene backbone. The rapid downshift of the ethylenic peak with a 180 fs time constant upon photoexcitation indicates that positive charge on the Schiff's base becomes immediately delocalized on the retinal polyene, consistent with transient absorption studies.[19] The blue-shift of the C=C stretch during the J to K transition also agrees with observed changes in the electronic absorption spectrum. This blue-shift indicates that the positive charge localizes back on the Schiff's base in the K intermediate, that is, the bond order of the C_{11}=C_{12} and C_{13}=C_{14} bonds is restored on the ∼3 ps time scale of 13-*cis* chromophore formation.

In the fingerprint region, the C−C stretch frequency has been suggested as a crucial marker band for the retinal configuration around the C_{13}=C_{14} bond based on both picosecond RR and IR spectroscopy on native and isotopically labeled bR.[21,34] The appearance of a broad band at 1189 cm^{-1}, distinct from the two ground state modes at 1170 and 1203 cm^{-1} suggests that a 13-*cis*-like configuration forms by 450 fs. However, we observe a further narrowing of the 1189 cm^{-1} band after 600 fs, which is assigned to formation of the 13-*cis* configuration in the K state. The band narrowing during the J to K transition could indicate either a reduction of conformational heterogeneity or further geometric changes such as torsional relaxation and vibrational cooling.

Broadband FSRS has the advantage of temporally probing the low frequency deformation modes that are coupled to the reaction coordinate. The C_{15}−H HOOP mode serves as a direct probe of the local torsion in the C_{14}−C_{15}=N region during the J to K transition. The absence of this HOOP feature in J suggests that this moiety is relatively planar. The delayed 3 ps rise in the HOOP intensity indicates that the geometrical changes induced by C_{13}=C_{14} photoisomerization are only complete in the K intermediate. The enhanced intensity of the HOOP mode in K presumably results from the appearance of distortion in the C_{14}−C_{15}=N moiety. This distortion may arise as a geometric consequence of the fully isomerized and planar 13-*cis* bond, that is, as the C_{13}=C_{14} bond assumes a planar geometry, the torsional strain induced on the backbone during the isomerization is transferred to the C_{14}−C_{15} bond.

The 150 fs delayed onset of the J state FSRS signals shows that reactive internal conversion does not begin immediately after Franck−Condon excitation. The femtosecond actinic pulse induces simultaneous population changes in the ground and excited state. Any TA or FSRS signals that result from the Franck−Condon state must appear with no delay and hence exhibit a 50% rise at $t = 0$. The delayed rise of the J FSRS signals in Figure 5 is consistent with earlier 800 nm FSRS data revealing a ∼250 fs excited state emission feature. We did not observe any vibrational signature of I_{460} dynamics on the excited state possibly due to the short intrinsic lifetime of this fleeting intermediate. The 150 fs dwell before the appearance of the red-shifted ethylenic mode in J demonstrates that significant excited state evolution must occur before the system reaches the reactive region or conical intersection in phase space where it collapses to J with little additional delay. A fast delay component (∼150 fs) was also seen in transient absorption dynamics in the 650−800 nm region at low photon flux. It was presumed that the instantaneous rise of the stimulated emission

corresponded to fast internal conversion on the excited state.[40,41] Thus our measurements are consistent with multimode evolution on a single electronic surface which precedes the reactive conical intersection.

In conclusion, the unique ability of tunable FSRS to obtain resonance Raman vibrational spectra of the birth of the J and K intermediates has enabled us to characterize the initial reaction dynamics during the bR photocycle. The overall photoisomerization mechanism can be summarized: After photoexcitation, charge transfer from the Schiff's base to the polyene backbone is complete by 180 fs. The light-induced electronic change initiates excited state wavepacket motion that propagates until the reactive internal conversion channel is reached from which the J ground state photoproduct is formed in 450 fs. The rise of the fully isomerized ground state intermediate K in ∼4 ps is characterized by the appearance of a blue-shifted C═C stretch and a distinct C_{15}−H HOOP mode, thereby indicating the relocalization of the positive charge on the Schiff's base and the production of a C_{14}−C_{15} distortion, respectively. The completion of the *all-trans* to 13-*cis* isomerization process subsequently drives the elementary steps of the proton translocation process across the membrane.

Acknowledgment. We thank Prof. Roberto Bogomolni for providing bR samples. We also thank Renee Frontiera for stimulating discussions on the resonance FSRS process. This work was supported by the Mathies Royalty fund and partly by the U.S.−Israel Binational Science Foundation (BSF) grant (2006400).

Supporting Information Available: Plot of the temporal dynamics of ground state bleaching and complete ref 4. This material is available free of charge via the Internet at http://pubs.acs.org.

JA809137X

(40) Schmidt, B.; Sobotta, C.; Heinz, B.; Laimgruber, S.; Braun, M.; Gilch, P. *Biochim. Biophys. Acta Bioenerg.* **2005**, *1706*, 165–173.
(41) Ruhman, S.; Hou, B. X.; Friedman, N.; Ottolenghi, M.; Sheves, M. *J. Am. Chem. Soc.* **2002**, *124*, 8854–8858.